

Unexpected C–C Bond Formation with a Ferrocenyl Fischer Carbene Complex

Philipp Veit,^[a] Sebastian Seibert,^[a] Christoph Förster,^{*[a]} and Katja Heinze^{*[a]}

Dedicated to Prof. Manfred Scheer on the Occasion of his 65th Birthday

Abstract. Thermolysis of $(OC)_5Cr(C(OEt)(Fc))$ (**1**) gives 2,*N*-difero-cenyl acetamide $Fc-CH_2-CO-NH-Fc$ (**2**) in the presence of amino ferrocene $Fc-NH_2$. In the absence of a nucleophile, 4-ethoxy-2,3,4-triferrocenyl-cyclobut-2-enone (**3**) forms from **1** under thermal activation. Single crystal X-ray diffraction, NMR spectroscopy and mass

spectrometry unambiguously confirm the structure of both unexpected products. Quantum chemical calculations and kinetic experiments by mass spectrometry and IR spectroscopy help to propose conceivable pathways to their formation.

Introduction

Fischer carbene complexes of group 6 metals^[1] display a highly versatile follow-up chemistry (Scheme 1). This field has matured into well-established applications in organic synthesis.^[2–6] For example, treating vinyl or aryl-substituted alkoxy carbenes with alkynes yields phenols and naphthols, respectively (Scheme 1a, Dötz benzannulation reaction).^[7–13] Carbenes with 1,3-difluorophenyl-, cyclopropyl or ferrocenyl substituents furnish cyclobutenones (or cyclopentenones) in the presence of alkynes (Scheme 1a, Zora).^[14–21]

In these cases, the initial steps comprise CO dissociation from the carbene complex. Hence, thermal activation is typically required. Coordination of the alkyne and insertion of the alkyne into the metal-carbene bond gives a vinyl carbene complex. CO insertion forms a vinyl ketene coordinated by a $Cr(CO)_3$ fragment. From this intermediate, the Dötz products ($R = \text{aryl or vinyl}$) or the cyclobutenones ($R = \text{cyclopropyl}$, Scheme 1a, Zora) evolve.

A classical reaction of alkoxy Fischer carbenes is the nucleophilic substitution of the alkoxide by primary or secondary amines giving the corresponding aminocarbene complexes (Scheme 1b).^[22,23] However, using amino ferrocene $Fc-NH_2$ ^[24,25] as nucleophile and the carbene complex

$(OC)_5Cr(C(OEt)(Fc))$ (**1** ($R^1 = Et$, $R^2 = Fc$), the expected difero-cenyl carbene complex $(OC)_5Cr(C(NHFc)(Fc))$ could not be obtained.^[26] The low nucleophilicity of $Fc-NH_2$ might be responsible for this failure. However, increasing the nucleophilicity of $Fc-NH_2$ by deprotonation with potassium hexamethyldisilazide resulted in the successful formation of $(OC)_5Cr(C(NHFc)(Fc))$ (Scheme 1c).^[26]

On the other hand, using lithium morpholin-4-ide and alkoxy carbene complexes with bulky substituents ($R^1 = \text{menthyl}$, Scheme 1) results in a C–C coupling reaction to give α -alkoxy acetamides presumably via biscarbenes (Scheme 1d).^[27] In the absence of a nucleophile or alkyne, simple thermolysis of carbene complexes yields the olefin as formal carbene-carbene coupling product as already reported by Fischer (Scheme 1e).^[28,29]

In this study, we show that the thermally activated reaction of **1** with the weak nucleophile $Fc-NH_2$ gives 2,*N*-difero-cenyl acetamide $Fc-CH_2-CO-NH-Fc$ (**2**) (Scheme 1f) instead of the initially intended (amino ferrocenyl)(ferrocenyl)carbene complex^[26] (Scheme 1c). Beyond this thermal pathway, the photo-induced formation of a related compound $MeOOC-CH_2-(\eta^5-C_5H_4)Re(CO)_3$ of the Fischer carbene complex $(OC)_5Cr(C(OMe)(\eta^5-C_5H_4)Re(CO)_3)$ with MeOH had been reported by Sierra.^[30] Obviously, the C–C coupling product **2** arises from two C_1 building blocks (carbene and CO). From the analogous reaction of the carbene complex **1** and adamantylamine only traces of the corresponding C–C coupling product 2-ferrocenyl-*N*-adamantyl acetamide $Fc-CH_2-CO-NH-Ad$ (**2^{Ad}**) are detected. Instead, the triferrocenyl-substituted cyclobutenone **3** forms in significant amounts (Scheme 1g). **3** is obviously a C–C coupling product arising formally from four C_1 building blocks, namely from three ferrocenyl carbenes and CO. Cyclobutenone **3** even forms in the absence of adamantylamine by simple heating.

To the best of our knowledge, the formation of acetic acid derivatives by weak nucleophiles and the thermally induced formation of cyclobutenones from carbene complexes in the ab-

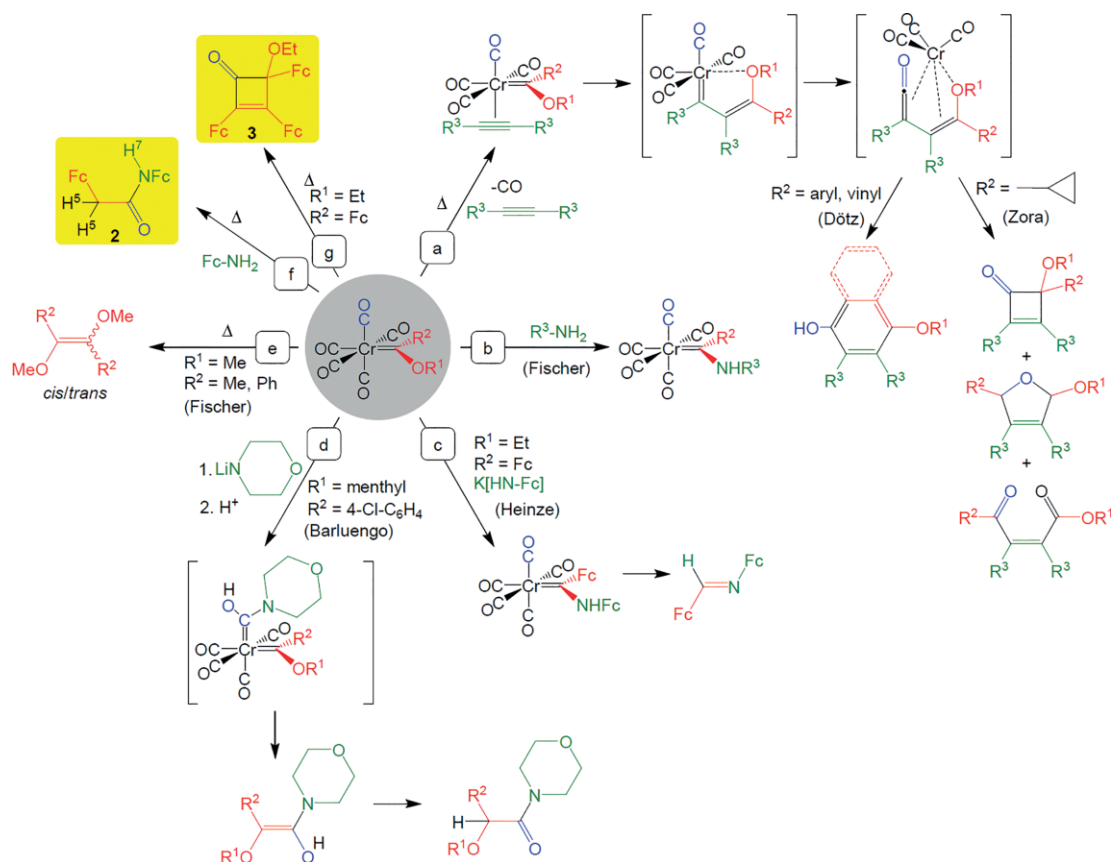
* Dr. C. Förster
E-Mail: cfoerster@uni-mainz.de,

* Prof. Dr. K. Heinze
E-Mail: katja.heinze@uni-mainz.de

[a] Department of Chemistry
Johannes Gutenberg University of Mainz
Duesbergweg 10–14
55128 Mainz, Germany

Supporting information for this article is available on the WWW under <http://dx.doi.org/10.1002/zaac.201900350> or from the author.

© 2020 The Authors. Published by Wiley-VCH Verlag GmbH & Co. KGaA. • This is an open access article under the terms of the Creative Commons Attribution-NonCommercial-NoDerivs License, which permits use and distribution in any medium, provided the original work is properly cited, the use is non-commercial and no modifications or adaptations are made.



Scheme 1. Reactivity of chromium carbene complexes, which is relevant to this study.

sence of alkynes by formal coupling of CO and one and three carbene building blocks, respectively, have not been reported so far. Hence, we present our initial results on these unexpected C-C coupling reactions and discuss conceivable mechanistic aspects in the context of the well-established reactivity of Fischer carbene complexes.

Results and Discussion

Synthesis and Characterization of **2**

The ferrocenyl-substituted chromium carbene complex **1** (prepared according to literature procedures)^[26,31–33] was treated with amino ferrocene Fc-NH₂^[24,25] in toluene under reflux. After chromatographic workup, a brown solid was isolated and characterized (Figures S1–S4, Supporting Information).

Instead of the anticipated substituted carbene complex (OC)₅Cr(C(NHFc)(Fc)),^[26] the acetic acid derivative **2** was isolated in 14% yield. Single crystals of **2** were obtained and the solid-state structure was determined by X-ray diffraction (Figure 1a). **2** crystallizes in the orthorhombic space group *Pbca* with one molecule in the asymmetric unit (Figure 1a). Selected bond lengths, bond angles and dihedral angles of the single-crystal X-ray diffraction data and the corresponding Density Functional Theory (DFT) calculation are collected in Table S1 (Supporting Information). The metrical data of the

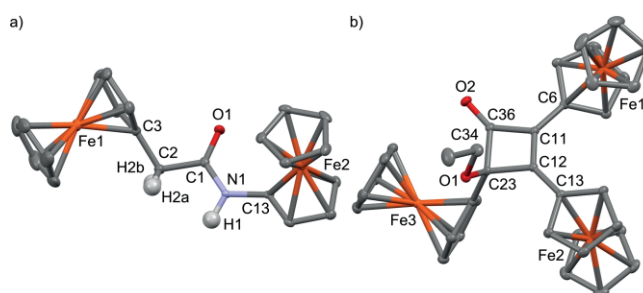


Figure 1. Molecular structures of (a) **2** and (b) **3** from single crystal XRD (hydrogen atoms are omitted for clarity except for NH and CH₂, thermal ellipsoids at 30% probability).

ferrocenyl moieties are unremarkable. The amides are linked by N–H⋯O=C hydrogen bonds between adjacent molecules [*d*(N⋯O) 2.894(5) Å] giving linear hydrogen bonded chains as commonly observed in ferrocenyl amides.^[25,34–35] In the solid state, the characteristic amide-A, amide-I and amide-II bands for hydrogen-bonded amides appear at 3280, 1659, 1566 cm^{−1} in a similar range to those of Fc-NHCOCH₃ (3262, 1655, 1580 cm^{−1}).^[25] In CD₂Cl₂ solution the chains disassemble into monomers as shown by the ¹H NMR resonance of the amide proton at δ_{H7} = 6.74 ppm (see Scheme 1 for atom numbering). In [D₈]THF, solvent coordinates to the amide (δ_{H7} = 8.23 ppm). The most unexpected observation is the presence of the additional CH₂ group in the molecule (Figure 1a). The

methylene group is furthermore confirmed by its proton resonance at ($\delta_{\text{H5}} = 3.33$ ppm in CD_2Cl_2 ; see Scheme 1 for atom numbering), the characteristic CH_2 stretching vibration at 2960 cm^{-1} and the FD mass spectrum of **2** ($m/z = 427$).

As this compound can be obtained by a much simpler route e.g. from ferrocenyl acetic acid and amino ferrocene using conventional amide coupling reactions^[25,34–40] as described in the Supporting Information (experimental procedure, Figures S19–S21, Supporting Information), no attempts to optimize this reaction were undertaken. However, the CH_2 group formation from the initial carbene ligand is unusual and will be discussed next.

Mechanistic Considerations on the Formation of **2**

As the *N*-ferrocenyl group is bound to a carbonyl group in the final product, nucleophilic attack of Fc-NH_2 onto a *cis*-CO ligand at **1** is highly probable. Indeed, biscarbene complexes have been reported by Fischer using $\text{M}(\text{CO})_6$ and LiPMe_2 after methylation in very low yield.^[41] More recently, Barluenga succeeded in isolating biscarbene complexes starting from chromium and tungsten alkoxy carbenes and strong heteronucleophiles such as amides or alkoxides after alkylation (Scheme 1d).^[27] Heating these (aminoaryl)(alkoxyalkenyl)-biscarbene tungsten complexes to $35\text{ }^\circ\text{C}$ furnished the olefinic carbene-carbene coupling products in good yields (Scheme 1d).^[27]

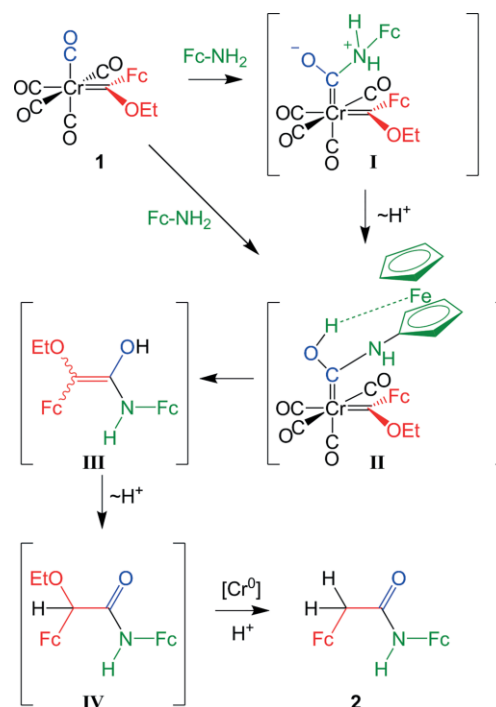
A fully analogous reaction (without the intermediate alkylation step) might be operative here. Amino ferrocene, although a weak nucleophile, attacks a carbonyl ligand *cis* to the carbene ligand forming zwitterion **I** (Scheme 2). After tautomerization intermediate **II** forms. According to quantum chemical calculations, the resulting OH group forms a hydrogen bond to the ferrocenyl iron(II) center Fe2 of the initial amino ferrocene in intermediate **II** irrespective of the conformation (Figure 2). Possibly, **II** can also form directly from Fc-NH_2 **1** assisted by the evolving $\text{O1H1}\cdots\text{Fe2}$ hydrogen bond. $\text{XH}\cdots\text{Fe}$ hydrogen bonds are meanwhile a well-established structural motif.^[26,42–45] The $\text{XH}\cdots\text{Fe}$ bond dissociation energy can amount up to $13\text{ kJ}\cdot\text{mol}^{-1}$. Consequently, the ferrocenyl moiety might assist the nucleophilic attack acting as an internal base.^[46]

After carbene-carbene coupling as the key C–C bond forming step, enol **III** forms (Scheme 2). Enol **III** would then tautomerize to the by $82\text{ kJ}\cdot\text{mol}^{-1}$ more stable amide **IV** according to DFT calculations (Scheme 2 and Figure S5, Supporting Information).

Under the inert conditions employed, the chromium(0) species could be competent to reduce the alkoxy derivative **IV** to the final product **2** accounting for the formation of the CH_2 group. Indeed, secondary desalkoxylation reactions with chromium(0) carbenes have been reported in several cases,^[47–50] likely forming chromium(II) alkoxides.^[51–54]

Synthesis and Characterization of **3**

To shed light onto the role of the incoming amine in the reaction discussed above, Fc-NH_2 was replaced by the bulky,



Scheme 2. Proposed mechanism for the formation of **2** via biscarbenes, carbene-carbene coupling and reduction.

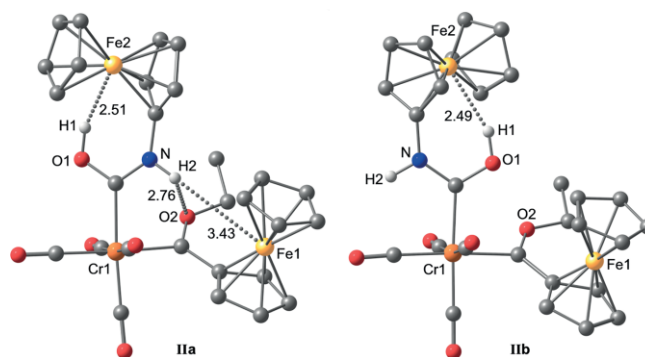


Figure 2. DFT optimized biscarbene intermediate **II** (distances given in Å). Conformer **IIa** is only slightly stabilized by $4\text{ kJ}\cdot\text{mol}^{-1}$ with respect to **IIb**.

more nucleophilic adamantylamine Ad-NH_2 in the reaction with **1**. Naturally, Ad-NH_2 is incompetent to form an intramolecular, possibly rate-enhancing $\text{O1H1}\cdots\text{Fe2}$ hydrogen bond.

In fact, only traces of the expected adamantyl derivative $\text{Ad-NHCO-CH}_2\text{-Fc}$ (**2^{Ad}**) were detected by FD mass spectrometry ($m/z = 377$; Figure S6, Supporting Information) of the reaction mixture. Instead, the triferrocenyl cyclobutenone derivatives 4-ethoxy-2,3,4-triferrocenyl-cyclobut-2-enone (**3**; $m/z = 664$) and 4-(adamantylamide)-2,3,4-triferrocenyl-cyclobut-2-enone (**3^{Ad}**; $m/z = 770$) were identified (Figure S6, Supporting Information). The former was successfully isolated from the reaction mixture and characterized (Figures S7–S14, Supporting Information). Obviously, the amine was not incorporated into **3** in spite of its higher nucleophilicity. While Ad-NH_2 fails to attack a CO ligand of **1** at a significant rate, the

assisting O1H1...Fe2 hydrogen bond (Figure 2) might be responsible for the special reactivity of Fc-NH₂ allowing its attack on the CO ligand.

As Ad-NH₂ appears non-essential for the formation of **3**, thermolysis of **1** was performed in the absence of any nucleophile. Indeed, in the FD mass spectrum of the reaction mixture, a peak at $m/z = 664$ appears corresponding to the molecular mass of **3** along with peaks assignable to carbene coupling products ($m/z = 440, 442, 484$) and traces of an oxidation product of **3** ($m/z = 680$). The latter might be assigned to a ring-opened keto ester 2,3,4-triferrocenyl-4-oxo-but-2-enoic acid ethyl ester (Scheme 1a, Zora pathway; with R¹ = Et, R² = R³ = Fc). After chromatographic workup, cyclobutenone **3** was isolated in a remarkable 17% yield considering the formation of four C-C bonds in a single reaction.

Compound **3** crystallizes in the monoclinic space group *P2₁/c* with one molecule in the asymmetric unit (Figure 1b) without significant intermolecular contacts. Table S2 (Supporting Information) reports selected bond lengths, bond angles and dihedral angles of the single-crystal X-ray diffraction data and the corresponding DFT calculation. The cyclobutenone ring is essentially planar, the C=C double bond [1.378(2) Å] is slightly longer than that found in the four other crystallographically characterized cyclobutenones with an alkoxy substituent (1.353–1.368 Å).^[55–58] The Cp rings of the Fc substituents at the C=C double bond are quite coplanar to the four-membered ring (torsion angles C=C-C_{ipso}-C_{alpha} = 9.2° and 17.1°). The three bulky ferrocenyl substituents at the 2, 3 and 4 positions point up, down and down, respectively, relative to the cyclobutenone plane avoiding steric hindrance.

The ¹H and ¹³C{¹H} NMR spectra exhibit all expected resonances of the chemically different ferrocenyl substituents although complete individual assignment was impossible (Figures S7–S12, Supporting Information). The CH₂ group of the ethoxy substituent possesses diastereotopic protons resulting in two doublets of quartets in the ¹H NMR spectrum. In the solid state and in heptane, the absorption band of the C=O stretching vibration appears at 1738 and 1751 cm⁻¹, respectively (Figure S13, Supporting Information). The value in the solid is rather low compared to the reported range for cyclobutenones (solid: 1757–1760 cm⁻¹ solid, CDCl₃: 1753–1758 cm⁻¹).^[14–18] Two intramolecular short CH...O distances of 2.90 and 2.81 Å, namely from the 2-ferrocenyl (α -CH) and 4-ferrocenyl (unsubstituted Cp-H) substituent, might be responsible for this finding especially in the solid state. According to quantum chemical calculations, these CH stretches indeed couple to the carbonyl stretching vibration (Figure S15, Supporting Information).

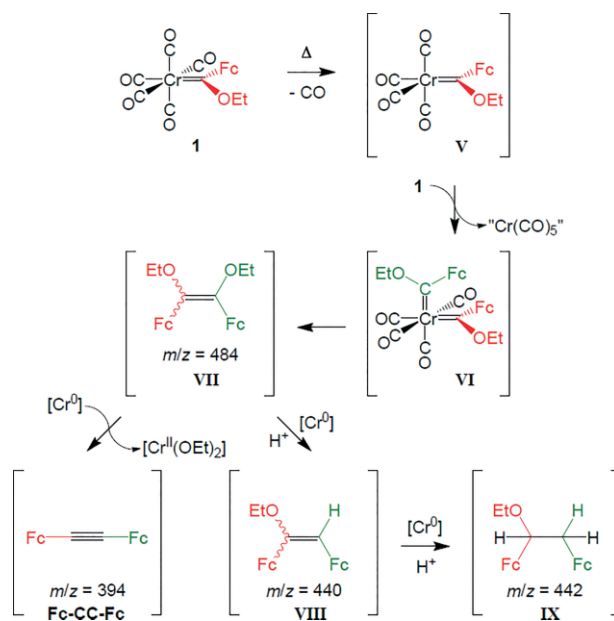
The three chemically different ferrocenyl substituents of **3** give rise to three individual quasi-reversible one-electron redox waves in the cyclic voltammogram at -80, 140 and 340 mV vs. the ferrocene/ferrocenium couple under our conditions (Figure S16, Supporting Information). Assignment of the oxidation processes to individual ferrocenes is impossible at this stage.

A conceivable mechanism to the formation of **3** is discussed next.

Mechanistic Considerations on the Formation of **3**

In a formal retrosynthesis, the triferrocenyl cyclobutenone derivative **3** can be derived from a CO unit and three ferrocenyl carbenes (under partial desalkoxylation). As cyclobutenones are accessible from alkynes and Fischer carbene complexes (lacking conjugated aryl or vinyl carbene substituents which would enable the Dötz reaction, Scheme 1a) according to previous work by Zora and co-workers (Scheme 1a), the formation of **3** from **1** might be traced back to a thermally induced formation of the required diferrocenyl alkyne Fc-C≡C-Fc.^[14–21]

Fischer reported the formation of carbene-carbene coupling products, i.e. *cis/trans*-dimethoxy stilbene and *cis/trans*-dimethoxy 2-butene, by thermolysis of chromium methoxy carbenes (Scheme 1e).^[28,29] Similarly, heating **1** in toluene releases CO giving the unsaturated complex **V** (Scheme 3). Carbene transfer from **1** then could form biscarbene **VI**. Carbene-carbene coupling releases *cis/trans*-1,2-diethoxy-1,2-diferrocenyl ethylene **VII** (Scheme 3) which has been identified by a peak in the FD mass spectrum ($m/z = 484$; Figure 3).



Scheme 3. Proposed mechanism for formation of 1,2-diferrocenyl alkenes **VII** and **VIII**, 1,2-diferrocenyl alkane **IX**, and diferrocenyl alkyne Fc-C≡C-Fc.

Furthermore, peaks at $m/z = 440$ and 442 are observed which can be assigned to *cis/trans*-1-ethoxy-1,2-diferrocenyl ethylene **VIII** and 1-ethoxy-1,2-diferrocenyl ethane **IX**, respectively (Figure 3). **VIII** could form via secondary desalkoxylation of **VII** by chromium(0) species similar to the proposed desalkoxylation of **IV** (Scheme 2) and literature precedents.^[47–50] Further reduction of **VIII** then leads to the alkane **IX**. The latter is a dead-end in the reaction to **3** and indeed accumulates during the reaction, while **VII** and **VIII** are consumed over time (Figure 3). Concomitantly, the peak for the product **3** increases. The proposed diferrocenyl alkyne could form directly from diethoxy alkene **VII** with

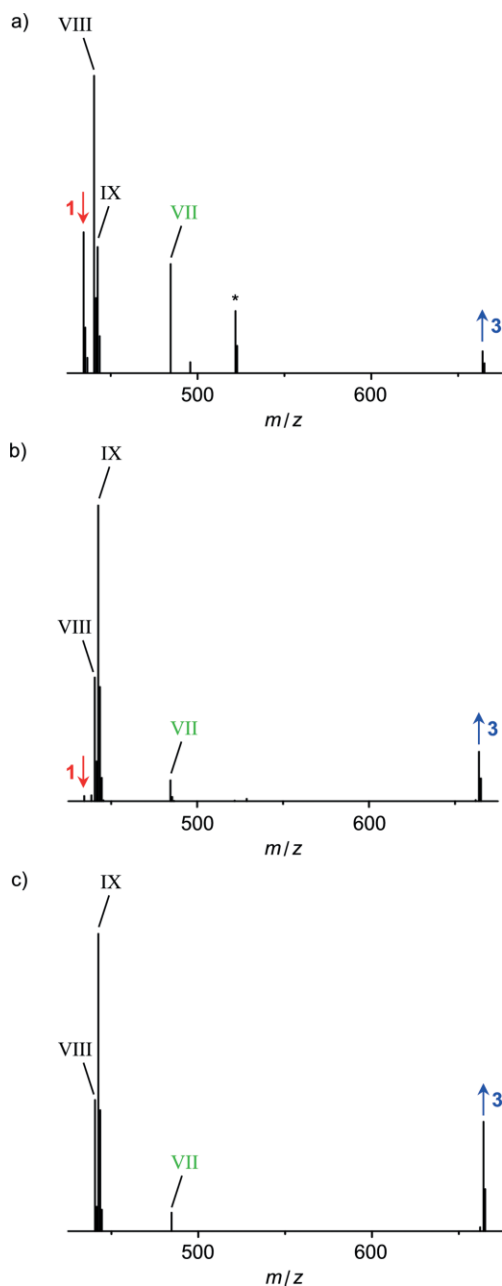
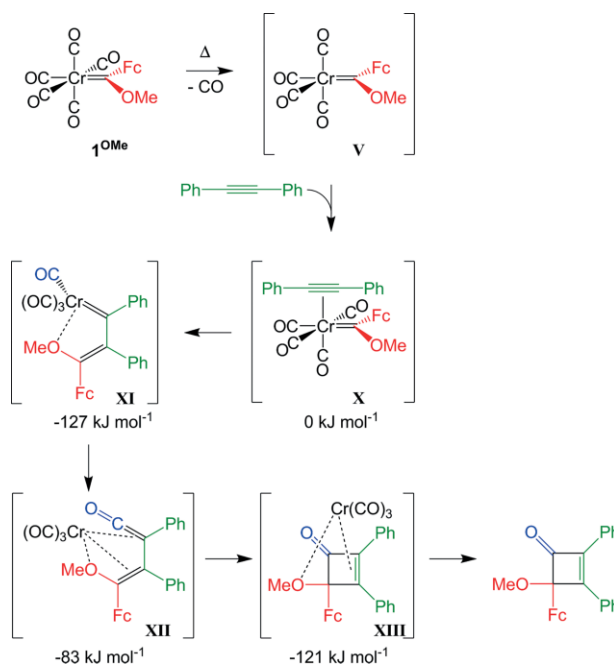


Figure 3. LIFDI mass spectra taken during the thermolysis of **1** after (a) 1 d, (b) 2 d, and (c) 8 d in toluene at 111 °C (* = unknown intermediate).

chromium(0) species^[47–50] generating chromium(II) alkoxides.^[51–54] However, $\text{Fc-C}\equiv\text{C-Fc}$ ($m/z = 394$) is not observed by mass spectrometry during the reaction. Possibly, the formed alkyne reacts too fast with the unsaturated chromium carbene $(\text{OC})_4\text{Cr}(\text{C}(\text{OEt})(\text{Fc}))$ **V** (Scheme 3) to accumulate significantly in the reaction mixture. The alkyne complex then evolves further to the cyclobutenone **3** according to Zora's studies (Scheme 1a).^[19–21] In agreement with the proposed fast reaction, tetracarbonyl chromium complex **V** could not be detected by mass spectrometry and IR spectroscopy (in *n*-heptane) during the thermolysis of **1**. IR spectra acquired during the thermolysis merely display absorption bands assignable to

$\text{Cr}(\text{CO})_6$ (1988 cm^{-1}) and **VII** (1724 cm^{-1})^[59] (Figure S17, Supporting Information).

In a computational model reaction of the methoxy substituted carbene complex **1^{OMe}** with toluene we studied the course of the reaction towards the corresponding cyclobutenone (Scheme 4, Figure S18, Supporting Information). After CO loss, the alkyne coordinates to **V** giving the alkyne complex **X**. The toluene complex evolves to the thermodynamically preferred vinyl carbene complex **XI**. Coordination of the alkoxide substituent stabilizes the unsaturated chromium center in **XI** which evolves to the $\text{Cr}(\text{CO})_3$ coordinated vinyl ketene^[60–61] **XII**. Finally, ring closure yields the $\text{Cr}(\text{CO})_3$ coordinated cyclobutenone **XIII**.



Scheme 4. Computational model reaction of **1^{OMe}** and $\text{Ph-C}\equiv\text{C-Ph}$. Relative energies of **X**, **XI**, **XII**, and **XIII** from the DFT calculations.

Conclusions

Products of carbene-carbene coupling reactions have been obtained by thermolysis of $(\text{OC})_5\text{Cr}(\text{C}(\text{OEt})(\text{Fc}))$ (**1**). In the presence of amino ferrocene Fc-NH_2 , 2,*N*-diferrocenyl acetamide $\text{Fc-CH}_2\text{-CO-NH-Fc}$ (**2**) was isolated. The initial attack of the rather weak nucleophile Fc-NH_2 at a CO ligand of **1** is possibly assisted by an $\text{OH}\cdots\text{Fe}$ hydrogen bond. In the absence of a nucleophile, CO dissociation, carbene transfer and carbene-carbene coupling yields diferrocenyl ethylenes, diferrocenyl ethane and possibly diferrocenyl alkyne. The diferrocenyl alkyne coordinates to **1** after CO dissociation. Alkyne and CO insertion finally releases 4-ethoxy-2,3,4-triferrocenylcyclobut-2-enone **3**. Key reactions in both scenarios are the intermediate formation of biscarbene complexes and carbene-carbene coupling.

Experimental Section

General Procedures: All reactions were performed in an argon atmosphere unless otherwise noted. A glovebox of the type UniLab/MBraun (Ar 4.8, O₂ < 1 ppm, H₂O < 1 ppm) was used for storage and weighing of sensitive compounds. All samples that required the absence of oxygen were prepared in the same glovebox. Dichloromethane was dried with CaH₂ and distilled prior to use. THF, xylenes and toluene were distilled from potassium. *n*-Heptane was dried with molecular sieves 4 Å for at least 48 h. Deuterated solvents were purchased from euriso-top. 1-Adamantylamine was received from Alfa Aesar. **1** [26,31–33] and amino ferrocene^[24,25] were synthesized using literature procedures. NMR spectra were recorded on a Bruker Avance DRX 400 spectrometer at 400.31 MHz (¹H) and 100.07 MHz (¹³C{¹H}). All resonances are reported in ppm vs. the solvent signal as internal standard. CD₂Cl₂ (¹H: δ = 5.32 ppm; ¹³C: δ = 54.0 ppm), [D₈]THF (¹H: δ = 1.72, 3.58 ppm).^[62] IR spectra were recorded with a Bruker ALPHA II FT-IR spectrometer with a platinum Di-ATR module as solid state samples or in *n*-heptane with a transmission module using KBr cells. UV/Vis/NIR spectra were recorded on a Varian Cary 5000 spectrometer by using 1.0 cm cells (Hellma, suprasil). Electrochemical experiments were carried out on a BioLogic SP-200 voltammetric analyzer using platinum wires as counter and working electrodes and a 0.01 M Ag/AgNO₃ electrode as reference electrode. Cyclic voltammetry measurements were carried out at scan rate of 100 mV·s⁻¹ using 0.1 M [*n*Bu₄N][PF₆] as supporting electrolyte in CH₂Cl₂. Potentials are referenced to the decamethylferrocene/decamethylferrocenium couple (*E*_{1/2} = -270 ± 5 mV under the experimental conditions; literature value *E*_{1/2} = -590 mV vs. ferrocene^[63]) and given vs. ferrocene. FD mass spectra were recorded on a Thermo Fisher DFS mass spectrometer with a LIFDI upgrade. Elemental analyses were performed by the microanalytical laboratory of the department of chemistry, University of Mainz.

Density Functional Theory Calculations: DFT calculations were carried out using the ORCA program package (version 4.1.1).^[64] All calculations were performed using the B3LYP functional^[65–67] and employ the RIJCOSX approximation.^[68,69] Relativistic effects were calculated at the zeroth order regular approximation (ZORA) level.^[70] The ZORA keyword automatically invokes relativistically adjusted basis sets. To account for solvent effects, a conductor-like screening model (CPCM) modelling dichloromethane was used in all calculations.^[71,72] Geometry optimizations were performed using Ahlrichs' split-valence double- ξ basis set ZORA-def2-SVP which comprises polarization functions for all non-hydrogen atoms.^[73] Auxiliary basis set for General-purpose Coulomb fitting SARC/J decontracted def2/J up to Kr was used.^[74] Atom-pairwise dispersion correction was performed with the Becke-Johnson damping Scheme (D3BJ).^[75,76] The presence of energy minima was checked by numerical frequency calculations. The approximate free energies at 298 K were obtained through thermochemical analysis of the frequency calculation, using the thermal correction to the Gibbs free energy as reported by ORCA.

Crystal Structure Determination: Intensity data were collected with a Bruker AXS Smart1000 CCD diffractometer with an APEX II detector and an Oxford cooling system and corrected for absorption and other effects using Mo-*K*_α radiation (λ = 0.71073 Å). The diffraction frames were integrated using the SAINT package^[77] and most were corrected for absorption with MULABS^[78] of the PLATON software package.^[79] The structures were solved by direct methods and refined by the full-matrix method based on *F*² using the SHELXL software package.^[80,81] All non-hydrogen atoms were refined anisotropically while the positions of all hydrogen atoms were generated with appropriate geometric constraints and allowed to ride on their respective

parent carbon/nitrogen atoms with fixed isotropic thermal parameters. See Supporting Information for crystal data of **2** and **3**.

Crystallographic data (excluding structure factors) for the structures in this paper have been deposited with the Cambridge Crystallographic Data Centre, CCDC, 12 Union Road, Cambridge CB21EZ, UK. Copies of the data can be obtained free of charge on quoting the depository numbers CCDC-1962440 and CCDC-1962439. (Fax: +44-1223-336-033; E-Mail: deposit@ccdc.cam.ac.uk, http://www.ccdc.cam.ac.uk).

2,N-Diferrocenylacetamide (2): Amino ferrocene (422 mg, 2.1 mmol, 1.05 equiv.) and **1** (868 mg, 2.0 mmol, 1.0 equiv.) were heated under reflux in toluene (50 mL) for 120 h resulting in a dark solution and a dark precipitate. The reaction progress was monitored by TLC and LIFDI mass spectrometry. The solvent was removed under reduced pressure. Column chromatography (SiO₂, 42 × 3.5 cm, petroleum ether:THF, 6:4, *R*_f = 0.55) yielded a brown solid (119 mg, 0.28 mmol, 14%). **1**H NMR (CD₂Cl₂): δ = 6.74 (s, 1 H, H⁷), 4.50 (pt, 2 H, H⁹), 4.22 (pt, 4 H, H², H³), 4.18 (s, 5 H, H^{1/11}), 4.09 (s, 5 H, H^{1/11}), 3.96 (pt, 2 H, H¹⁰), 3.33 (s, 2 H, H⁵) ppm. **1**H NMR ([D₈]THF): δ = 8.23 (s, 1 H, H⁷), 4.61 (pt, 2 H, Cp(subst.)), 4.23 (pt, 2 H, Cp(subst.)) 4.12 (s, 5 H, H^{1/11}), 4.07 (pt, 2 H, Cp(subst.)), 4.05 (s, 5 H, H^{1/11}), 3.88 (pt, 2 H, Cp(subst.)), 3.17 (s, 2 H, H⁵) ppm. **MS** (FD): *m/z* (*int.* %) = 427.4 (100) [M⁺], 428.4 (30), 425.4 (9). Calcd. for C₂₂H₂₁Fe₂NO (427.0). **IR** (KBr): $\tilde{\nu}$ = 3280 (m), 3209 (sh), 3090 (m), 2960 (m), 2909 (w), 1659 (s), 1566 (s), 1481 (m), 1389 (m), 1265 (s), 1196 (m), 1096 (vs), 1026 (vs), 802 (vs), 710 (m), 494 (vs) cm⁻¹. **UV/Vis** (CH₂Cl₂): λ_{\max} (ε/M⁻¹ cm⁻¹) = 270 (1260), 335 (65) 440 (50) nm.

4-Ethoxy-2,3,4-triferrocenyl-cyclobut-2-enone (3): **1** (1302 mg, 3 mmol) was heated under reflux in xylenes (120 mL) for three days resulting in a dark solution and a dark precipitate. The reaction was monitored by TLC and LIFDI-MS. After removal of the solvent under reduced pressure, the crude reaction mixture dissolved in dichloromethane was filtered using a short celite pad. Column chromatography of 694 mg brown oil (SiO₂, 57 × 4.5 cm, CH₂Cl₂, *R*_f = 0.71) yielded a red solid (110 mg, 0.17 mmol, 17%). **1**H NMR (CD₂Cl₂): δ = 4.95 (pt, 2 H, C₅H₄), 4.80 (pt, 1 H, C₅H₄), 4.57 (pt, 1 H, C₅H₄), 4.55 (pt, 2 H, C₅H₄), 4.45 (pt, 2 H, C₅H₄), 4.28 (s, 5 H, Cp), 4.25 (s, 5 H, Cp), 4.24 (pt, 2 H, C₅H₄), 4.16 (pt, 1 H, C₅H₄), 4.08 (pt, 1 H, C₅H₄), 4.03 (s, 5 H, Cp), 3.67–3.60 (dq, ²J_{H,H} = 1.5, ³J_{H,H} = 7.0 Hz, 1 H, CH₂, H^{6b}), 3.54–3.47 (dq, ²J_{H,H} = 1.5, ³J_{H,H} = 7.0 Hz, 1 H, CH₂, H^{6a}), 1.25 (t, ³J(H,H) = 6 Hz, 3 H, CH₃) ppm. **13**C{¹H} NMR (CD₂Cl₂): δ = 191.24 (C¹⁰), 172.63 (C^{quat.}), 141.99 (C^{quat.}), 98.40 (C⁵), 87.81 (C^{quat.}), 72.93 (C^{quat.}), 72.53 (C^{quat.}), 72.35 (C^{Cp(subst.)}), 72.26 (C^{Cp(subst.)}), 70.88 (C^{Cp(subst.)}), 70.59 (C^{1/14/18}), 70.22 (C^{Cp(subst.)}), 70.15 (C^{Cp(subst.)}), 70.04 (C^{1/14/18}), 69.89 (C^{1/14/18}), 69.31 (C^{Cp(subst.)}), 69.01 (C^{Cp(subst.)}), 68.85 (C^{Cp(subst.)}), 68.26 (C^{Cp(subst.)}), 68.17 (C^{Cp(subst.)}), 68.06 (C^{Cp(subst.)}), 66.82 (C^{Cp(subst.)}), 60.56 (C⁶), 16.2 (C⁷) ppm. **MS** (FD): *m/z* (*int.* %) = 663.9 (100) [M⁺], 664.9 (44), 662.0 (19), 665.9 (12), 662.9 (8). calcd. for C₃₆H₃₂Fe₃O₂ (664.05). **IR** (ATR): $\tilde{\nu}$ = 3088 (w), 2963 (m), 2917(w), 2870 (w), 2851 (w), 1738 (m), 1724 (sh), 1614 (m), 1482 (w), 1443 (w), 1410 (w), 1379 (w), 1336 (w), 1260 (vs), 1103 (s), 1074 (s), 1018 (s), 1004 (s), 917 (w), 864 (w), 794 (vs), 742 (sh), 695 (m), 474 (s) cm⁻¹. **IR** (*n*-heptane): $\tilde{\nu}$ = 1751 (w) cm⁻¹. **UV/Vis** (CH₂Cl₂): λ_{\max} (ε/M⁻¹ cm⁻¹) = 264 (12850), 321 (10850), 338 (sh, 2400), 489 (2450) nm. **CV** (CH₂Cl₂, vs. FcH/FcH⁺): *E*_{1/2} = -80, 140, 340 mV. C₃₆H₃₂Fe₃O₂ (664.05): calcd. C, 65.10; H, 4.86%; found: C, 64.73; H, 4.83%.

Supporting Information (see footnote on the first page of this article): spectroscopic data of **2** and **3**, alternative synthesis of **2**, cyclic

voltammogram of **3**, XRD data of **2** and **3**, additional DFT data and Cartesian coordinates of **2**, **3** and intermediates **Ia**, **Ib**, **III**, **IV**, **X**, **XI**, **XII**, **XII**.

Acknowledgements

We thank *Regine Jung-Pothmann* for collection of the diffraction data, *Dr. Mihail Mondeshki* for help with the NMR spectroscopic and LIFDI mass spectrometric experiments, *Taro Lieberth* for the independent synthesis of **2**, and the Johannes Gutenberg University of Mainz (Germany) for financial support to C. F. (Internal University Research Funding). DFT calculations were conducted using the supercomputer Mogon and advisory services offered by the Johannes Gutenberg University (www.hpc.uni-mainz.de), which is a member of the Gauss Alliance e.V. and the AHRP (Alliance for High Performance Computing in Rhineland Palatinate, www.ahrp.info). Open access funding enabled and organized by Projekt DEAL.

Keywords: Carbene complexes; Chromium; C–C coupling; Cyclobutenone / Ferrocene

References

- [1] E. O. Fischer, A. Maasböl, *Angew. Chem. Int. Ed. Engl.* **1964**, *3*, 580–581; *Angew. Chem.* **1964**, *76*, 645–646.
- [2] H. G. Raubenheimer, *Dalton Trans.* **2014**, *43*, 16959–16973.
- [3] D. I. Bezuidenhout, S. Lotz, D. C. Liles, B. van der Westhuizen, *Coord. Chem. Rev.* **2012**, *256*, 479–524.
- [4] a) M. A. Sierra, *Chem. Rev.* **2000**, *100*, 3591–3638; b) M. Gómez-Gallego, M. J. Mancheño, M. A. Sierra, *Acc. Chem. Res.* **2005**, *38*, 44–53.
- [5] K. H. Dötz, J. Stendel Jr., *Chem. Rev.* **2009**, *109*, 3227–3274.
- [6] a) J. Barluenga, M. A. Fernández-Rodríguez, E. Aguilar, *J. Organomet. Chem.* **2005**, *690*, 539–587; b) J. Barluenga, J. Flórez, F. J. Fañanás, *J. Organomet. Chem.* **2001**, *624*, 5–17; c) A. de Meijere, H. Schirmer, M. Deutsch, *Angew. Chem. Int. Ed.* **2000**, *39*, 3964–4002; *Angew. Chem.* **2000**, *112*, 4124–4162.
- [7] K. H. Dötz, *Angew. Chem. Int. Ed. Engl.* **1975**, *14*, 644–645; *Angew. Chem.* **1975**, *87*, 644–645.
- [8] L. Chupak in *Wiley Series on Comprehensive Name Reactions* (Eds.: E. J. Corey, J. J. Li), Wiley, Hoboken, N. J., **2010**, 197–422.
- [9] P. Hofmann, M. Hämmerle, *Angew. Chem. Int. Ed. Engl.* **1989**, *28*, 908–910; *Angew. Chem.* **1989**, *101*, 940–942.
- [10] H. Fischer, P. Hofmann, *Organometallics* **1999**, *18*, 2590–2592.
- [11] M. Torrent, M. Duran, M. Sol, *J. Am. Chem. Soc.* **1999**, *121*, 1309–1316.
- [12] P. G. Wenthold, M. A. Lipton, *J. Am. Chem. Soc.* **2000**, *122*, 9265–9270.
- [13] J. O. C. Jimenez-Halla, M. Solà, *Chem. Eur. J.* **2009**, *15*, 12503–12520.
- [14] K. H. Dötz, *J. Organomet. Chem.* **1977**, *140*, 177–186.
- [15] K. H. Dötz, W. Sturm, *J. Organomet. Chem.* **1986**, *310*, C22–C24.
- [16] K. S. Chan, G. A. Peterson, T. A. Brandvold, K. L. Faron, C. A. Challener, C. Hyldahl, W. D. Wulff, *J. Organomet. Chem.* **1987**, *334*, 9–56.
- [17] B. A. Anderson, J. Bao, T. A. Brandvold, C. A. Challener, W. D. Wulff, Y. C. Xu, A. L. Rheingold, *J. Am. Chem. Soc.* **1993**, *115*, 10671–10687.
- [18] J. Bao, W. D. Wulff, M. J. Fumo, E. B. Grant, D. P. Heller, M. C. Whitcomb, S.-M. Yeung, *J. Am. Chem. Soc.* **1996**, *118*, 2166–2181.
- [19] M. Zora, E. Ünsal Güngör, *Tetrahedron Lett.* **2001**, *42*, 4733–4735.
- [20] M. Zora, C. Açıkgöz, M. Odabaşoğlu, O. Büyükgüngör, *J. Organomet. Chem.* **2007**, *692*, 1571–1578.
- [21] M. Zora, T. Aslı Tumay, O. Büyükgüngör, *Tetrahedron* **2007**, *63*, 4018–4026.
- [22] a) E. O. Fischer, B. Heckl, H. Werner, *J. Organomet. Chem.* **1971**, *28*, 359–365; b) E. O. Fischer, M. Leupold, *Chem. Ber.* **1972**, *105*, 599–608.
- [23] D. B. Grotjahn, K. H. Dötz, *Synlett* **1991**, 381–390.
- [24] B. Bildstein, M. Malaun, H. Kopacka, K. Wurst, M. Mitterböck, K.-H. Ongania, G. Opromolla, P. Zanello, *Organometallics* **1999**, *18*, 4325–4336.
- [25] K. Heinze, M. Schlenker, *Eur. J. Inorg. Chem.* **2004**, 2974–2988.
- [26] P. Veit, C. Förster, S. Seibert, K. Heinze, *Z. Anorg. Allg. Chem.* **2015**, *641*, 2083–2092.
- [27] J. Barluenga, A. A. Trabanco, I. Pérez-Sánchez, R. de La Campa, J. Flórez, S. García-Granda, A. Aguirre, *Chem. Eur. J.* **2008**, *14*, 5401–5404.
- [28] E. O. Fischer, B. Heckl, K. H. Dötz, J. Müller, H. Werner, *J. Organomet. Chem.* **1969**, *16*, P29–P32.
- [29] E. O. Fischer, D. Plabst, *Chem. Ber.* **1974**, *107*, 3326–3331.
- [30] M. L. Lage, I. Fernández, M. J. Mancheño, M. Gómez-Gallego, M. A. Sierra, *Chem. Eur. J.* **2010**, *16*, 6616–6624.
- [31] a) J. G. López-Cortés, L. F. Contreras de la Cruz, M. C. Ortega-Alfaro, R. A. Toscano, C. Alvarez-Toledano, H. Rudler, *J. Organomet. Chem.* **2005**, *690*, 2229–2237; b) J. A. Connor, J. P. Lloyd, *J. Chem. Soc., Dalton Trans.* **1972**, 1470–1476.
- [32] D. I. Bezuidenhout, W. Barnard, B. van der Westhuizen, E. van der Watt, D. C. Liles, *Dalton Trans.* **2011**, *40*, 6711–6721.
- [33] G. A. Mose, E. O. Fischer, M. D. Rausch, *J. Organomet. Chem.* **1971**, *27*, 379–382.
- [34] K. Heinze, D. Siebler, *Z. Anorg. Allg. Chem.* **2007**, *633*, 2223–2233.
- [35] D. Siebler, M. Linseis, T. Gasi, L. M. Carrella, R. F. Winter, C. Förster, K. Heinze, *Chem. Eur. J.* **2011**, *17*, 4540–4551.
- [36] K. Heinze, K. Hempel, M. Beckmann, *Eur. J. Inorg. Chem.* **2006**, 2040–2050.
- [37] H. Huesmann, C. Förster, D. Siebler, T. Gasi, K. Heinze, *Organometallics* **2012**, *31*, 413–427.
- [38] A. Neidlinger, V. Ksenofontov, K. Heinze, *Organometallics* **2013**, *32*, 5955–5965.
- [39] J. Melomedov, J. R. Ochsmann, M. Meister, F. Laquai, K. Heinze, *Eur. J. Inorg. Chem.* **2014**, 1984–2001.
- [40] A. Neidlinger, C. Förster, K. Heinze, *Eur. J. Inorg. Chem.* **2016**, 1274–1286.
- [41] E. O. Fischer, F. R. Kreißl, C. G. Kreiter, E. W. Meineke, *Chem. Ber.* **1972**, *105*, 2558–2564.
- [42] C. Förster, P. Veit, V. Ksenofontov, K. Heinze, *Chem. Commun.* **2015**, *51*, 1514–1516.
- [43] T. Kienz, C. Förster, K. Heinze, *Organometallics* **2016**, *35*, 3681–3691.
- [44] P. Veit, E. Prantl, C. Förster, K. Heinze, *Organometallics* **2016**, *35*, 249–257.
- [45] K. Hanauer, M. T. Pham, C. Förster, K. Heinze, *Eur. J. Inorg. Chem.* **2017**, 433–445.
- [46] M. Malischewski, K. Seppelt, J. Sutter, F. W. Heinemann, B. Dittrich, K. Meyer, *Angew. Chem. Int. Ed.* **2017**, *56*, 13372–13376; *Angew. Chem.* **2017**, *129*, 13557–13561.
- [47] W. D. Wulff, R. W. Kaesler, G. A. Peterson, P.-C. Tang, *J. Am. Chem. Soc.* **1985**, *107*, 1060–1062.
- [48] S. U. Turner, J. W. Herndon, L. A. McMullen, *J. Am. Chem. Soc.* **1992**, *114*, 8394–8404.
- [49] M. Zora, J. W. Herndon, *Organometallics* **1993**, *12*, 248–249.
- [50] M. Zora, Y. Li, J. W. Herndon, *Organometallics* **1999**, *18*, 4429–4436.
- [51] J. J. H. Edema, S. Gambarotta, E. van Bolhuis, A. L. Spek, *J. Am. Chem. Soc.* **1989**, *111*, 2142–2147.
- [52] O. L. Sydora, D. S. Kuiper, P. T. Wolczanski, E. B. Lobkovsky, A. Dinescu, T. R. Cundari, *Inorg. Chem.* **2006**, *45*, 2008–2021.
- [53] P. Qiu, R. Cheng, B. Liu, B. Tumanskii, R. J. Batrice, M. Botoshansky, M. S. Eisen, *Organometallics* **2011**, *30*, 2144–2148.
- [54] M. Yousif, A. C. Cabelof, P. D. Martin, R. L. Lord, S. Groysman, *Dalton Trans.* **2016**, *45*, 9794–9804.

- [55] L. A. Paquette, L. H. Kuo, J. Tae, *J. Org. Chem.* **1998**, *63*, 2010–2021.
- [56] S. Iwata, T. Hamura, K. Suzuki, *Chem. Commun.* **2010**, *46*, 5316–5318.
- [57] M. W. Davies, J. P. A. Harrity, C. N. Johnson, *Chem. Commun.* **1999**, 2107–2108.
- [58] A. R. Hergueta, H. W. Moore, *J. Org. Chem.* **2002**, *67*, 1388–1391.
- [59] M. L. Lage, D. Curiel, I. Fernández, M. J. Mancheño, M. Gómez-Gallego, P. Molina, M. A. Sierra, *Organometallics* **2011**, *30*, 1794–1803.
- [60] M. A. Huffman, L. S. Liebeskind, W. T. Pennington, *Organometallics* **1992**, *11*, 255–266.
- [61] M. A. Huffman, L. S. Liebeskind, *J. Am. Chem. Soc.* **1990**, *112*, 8617–8618.
- [62] G. R. Fulmer, A. J. M. Miller, N. H. Sherden, H. E. Gottlieb, A. Nudelman, B. M. Stoltz, J. E. Bercaw, K. I. Goldberg, *Organometallics* **2010**, *29*, 2176–2179.
- [63] N. G. Connelly, W. E. Geiger, *Chem. Rev.* **1996**, *96*, 877–910.
- [64] F. Neese, *WIREs Comput. Mol. Sci.* **2012**, *2*, 73–78.
- [65] A. D. Becke, *J. Chem. Phys.* **1993**, *98*, 5648–5652.
- [66] C. Lee, W. Yang, R. G. Parr, *Phys. Rev. B* **1988**, *37*, 785–789.
- [67] B. Miehlich, A. Savin, H. Stoll, H. Preuss, *Chem. Phys. Lett.* **1989**, *157*, 200–206.
- [68] F. Neese, F. Wennmohs, A. Hansen, U. Becker, *Chem. Phys.* **2009**, *356*, 98–109.
- [69] R. Izsák, F. Neese, *J. Chem. Phys.* **2011**, *135*, 144105.
- [70] D. A. Pantazis, X.-Y. Chen, C. R. Landis, F. Neese, *J. Chem. Theory Comput.* **2008**, *4*, 908–919.
- [71] V. Barone, M. Cossi, *J. Phys. Chem. A* **1998**, *102*, 1995–2001.
- [72] S. Miertuš, E. Scrocco, J. Tomasi, *Chem. Phys.* **1981**, *55*, 117–129.
- [73] F. Weigend, R. Ahlrichs, *Phys. Chem. Chem. Phys.* **2005**, *7*, 3297–3305.
- [74] F. Weigend, *Phys. Chem. Chem. Phys.* **2006**, *8*, 1057–1065.
- [75] S. Grimme, J. Antony, S. Ehrlich, H. Krieg, *J. Chem. Phys.* **2010**, *132*, 154104.
- [76] S. Grimme, S. Ehrlich, L. Goerigk, *J. Comput. Chem.* **2011**, *32*, 1456–1465.
- [77] SMART Data Collection and SAINT-Plus Data Processing Software for the SMART System, Bruker Analytical X-ray Instruments, Inc.: Madison, WI **2000**.
- [78] R. H. Blessing, *Acta Crystallogr., Sect. A* **1995**, *51*, 33–38.
- [79] A. L. Spek, *Acta Crystallogr., Sect. D* **2009**, *65*, 148–155.
- [80] G. M. Sheldrick, *Acta Crystallogr., Sect. C* **2015**, *71*, 3–8.
- [81] G. M. Sheldrick, SHELXL-2014/7; University of Göttingen **2014**.

Received: December 20, 2019

Published Online: May 7, 2020